Received: 15th December 2024, Accepted: 16th December 2024, Published: 22nd December 2024

ANACHEM JOURNAL
ISSN: 2006-5221 (Online)

SILVER METAL NANOCOMPOSITE FROM AVOCADO PEAR SEED AS ADSORBENT FOR LEAD (II) IONS REMOVAL FROM AQUEOUS SOLUTION

E. O. Ofoma*[1], U. E. Ekpunobi[1], M. Ekeoma[2], C. I. Aghanwa[1]

[1]Department of Pure and Industrial Chemistry, Nnamdi Azikiwe University, Awka, Nigeria
[2]Department of Chemistry, Michael Okpara University of Agriculture Umudike, Nigeria
Corresponding author's e-mail: profchezzy@yahoo.com

DOI: https://doi.org/10.5281/zenodo.14567474

ABSTRACT

The present study aimed to investigate the adsorption behaviour of lead (II) ions from aqueous solutions using Avocado pear seed (APS) and silver metal nanocomposite (AgAPS)synthesized from Avocado pear seed. The agro waste underwent treatment processes such as chemical, physical and hydrothermal synthesis, giving rise to a nanocomposite with an enhanced surface area, structure and functional groups. The study investigated the influence of different parameters in adsorption, including pH, concentration, temperature, contact time and dosage. The thermodynamic studies, equilibrium isotherms, and kinetic information have been assessed. The functional groups, surface morphology, and crystalline nature of the APS and AgAPS adsorbents were analysed using Fourier transform infrared (FTIR), scanning electron microscope (SEM), and x-ray diffraction (XRD) techniques. The Langmuir and Freundlich adsorption models characterised the adsorption equilibrium isotherms. It was determined that the Langmuir adsorption model better fits the experimental data than the Freundlich models. The pseudo-second-order kinetic model can most accurately characterize the adsorption process.

Keywords: Adsorption, Avocado pear seed (APS), Lead, silver metal nanocomposite (AgAPS)

INTRODUCTION

According to Zhao *et al*., (2022), a regulatory relationship exists between economic growth, public health, and environmental pollution. Pollution is the foremost environmental factor contributing to the occurrence of diseases and early mortality globally in contemporary times. In 2015, it was estimated that diseases resulting from pollution accounted for around 9 million premature deaths globally, constituting 16% of the total number of deaths. This figure surpasses the combined death tolls of Acquired immune deficiency syndrome, Tuberculosis, and malaria by threefold. It exceeds the casualties caused by all types of violence and armed conflicts by a factor of 15 (Landrigan *et al.*, 2018).

According to a study by Shaddick *et al*. (2020), the World Health Organization (WHO) has estimated that approximately 4.2 million deaths annually can be attributed to outdoor air pollution. Xu *et al*., 2022) reported that approximately 80% of industrial and municipal wastewater is released into the environment without treatment, leading to

adverse consequences for human health and ecosystems. According to a study conducted by Landrigan *et al.*, (2018), the combined effects of air, water, and soil pollution resulted in the unfortunate demise of around 940,000 children globally in 2016. It is noteworthy that a significant proportion, precisely two-thirds, of these fatalities were children under the age of 5. Moreover, it is essential to highlight that most of these tragic incidents occurred in countries categorized as low- and middle-income economies. Industrial production can result in the emission of a range of harmful compounds, including organic and inorganic molecules, as well as toxic solvents and volatile organic chemicals. If these waste materials are discharged into aquatic ecosystems without sufficient treatment, they will contaminate water bodies (Chowdhary *et al*., 2020).

Over several decades, heavy metals have emerged as significant contributors to water contamination (Zaimee *et al*., 2021). In contemporary times, the prevailing pollutants that garner considerable attention and documentation are hazardous metals, specifically lead, cadmium, and mercury. These substances are generated as waste by diverse businesses and used batteries (Das and Raj, 2023). Lead poisoning claims the lives of approximately one million individuals annually. According to the World Health Organisation (WHO, 2022), a significant number of individuals, including a substantial proportion of children, are subjected to the detrimental effects of low levels of lead exposure. This exposure has been linked to many long-term health complications, including anaemia, hypertension, immunotoxicity, and reproductive organ toxicity. In their study, Guo *et al*., (2020) discovered that heavy metals, with a particular emphasis on Pb, present noncarcinogenic hazards to children and potential carcinogenic dangers to adults and children. These findings highlight the significant health risks individuals residing near mining and smelting regions face. Consequently, it is imperative to implement measures to regulate the release of heavy metals into the atmosphere. In addition to industrial solid waste, elevated concentrations of heavy metals in groundwater have been attributed to evaporation, anthropogenic activities, and the breakdown of rock formations, hence posing potential risks to human health (Karthikeyan *et al.*, 2021). Therefore, it is crucial to mitigate the presence of heavy metal pollution in the environment to an acceptable level.

Various techniques have been employed to remove heavy metals from wastewater, including membrane filtration, adsorption, and ion exchange. According to Denizil *et al*., (2022), adsorption is a highly effective method for purifying water that has been contaminated. In a recent study, Patel (2021), found that adsorption is a commonly employed method for removing pollutants. This technique offers several advantages, including high efficiency, cost-effectiveness, flexibility in design, availability of low-cost and user-friendly adsorbents worldwide, low energy requirements, and the ease of regenerating specifically used adsorbents. Adsorption processes are influenced by various parameters, such as temperature, pH, pollutant concentration, contact time, particle size, and the physical and chemical characteristics of the adsorbate and adsorbent (Fanourakis *et al*., 2020). According to Li *et*

al., (2020), the thermodynamic and kinetic investigations indicated that the adsorption process is characterized by exothermicity, spontaneity, and physisorption. Using agricultural waste plant materials to transform them into effective adsorbents is pertinent in mitigating pollution, particularly wastewater treatment (Yadav *et al*., 2021). A recent study by Božić *et al.,* (2021) demonstrated that beech sawdust and wheat straw exhibit favourable characteristics as adsorbents for removing lead ions from diluted aqueous solutions. According to Sonal and Mishra, (2021), it has been observed that plant waste adsorbents exhibit significant efficacy and can be subjected to different modifications depending on the specific pollutants being targeted. Plant adsorbents contain several functional groups, including acetamido, carbonyl, phenolic, structural polysaccharides, amido, amino, sulphydryl, carboxyl, alcohol, and esters. These functional groups exhibit an affinity for metal complexation, enabling them to effectively remove metal compounds from solutions (Sud *et al*., 2008).

While commercial activated carbons derived from plant waste have demonstrated efficacy in the removal of heavy metal ions and various contaminants, other adsorbents such as silica gels, zeolites, commercial alumina and ion-exchange resins have also exhibited notable success in this regard (Khan *et al*., 2023). However, it is essential to acknowledge that these adsorbents are not without their limits. Nanoparticles, a specific category of nanomaterials, have garnered significant attention in contemporary research across several industries due to their distinctive characteristics and extensive array of potential uses (Zuorro *et al*., 2019). According to Khan *et al.,* (2022), using plant extract in green nanotechnology presents a promising avenue for creating innovative nanoparticles possessing the necessary attributes for advancing biotechnology. Nanoparticles are favoured over alternative adsorbents owing to their numerous sorption sites, substantial specific surface area, capacity for low-temperature modification, porosity, surface functionalities, limited intraparticle diffusion distance, and ability to bind ions (Singh *et al*., 2018). Sadegh *et al.,* (2017) have presented a range of efficient, cost-effective, environmentally friendly nanomaterials with distinct functions. Some researchers have proposed using these nanomaterials to purify water supplies from industry to human consumption. The study conducted by Baran *et al*., (2020) demonstrated the efficacy of gold nanoparticles derived from *Capsicum annuum L*. leaves in removing hazardous metals from water samples.

Using plant waste to produce nanoparticles offers a potential solution for mitigating and controlling agricultural waste pollution (Sarkar *et al.,* 2021). An illustration of this may be seen in using agri-food waste extracts as reducing agents, which contributes to developing a sustainable system for synthesizing nanoparticles, particularly silver. This approach employs a green synthesis method and enhances the value of agri-food waste by incorporating it into the process. Moreover, the results indicate that utilizing agro-based adsorbents presents a viable substitute for non-agro-based adsorbents (Fagbayigbo *et al*., 2020). This study evaluates the viability of utilizing metal nanoparticles produced through the biosynthesis process using avocado pear seeds. The aim is to determine if these nanoparticles can be a more economical solution for mitigating lead contamination in

the environment undergoing filtration using agricultural waste materials.

MATERIALS AND METHODS

Plant Extraction

The avocado pear seeds were collected from a tree at Achina in Aguata, a local government in Anambra state. They were cut into smaller parts, washed with distilled water, and dried away from direct sunlight. The dried seeds were ground to fine size over a 40 mesh sieve and subjected to a 48-hour extraction process at room temperature using methanol as the solvent. Subsequently, the Whatman No.1 paper extracts resulted in crude extracts after concentration under reduced pressure (Djeussi *et al*., 2020).

Preparation of Silver Nanocomposite

$AgNO_3$ flakes were dissolved with distilled water to prepare 1M $AgNO_3$. Samples of the avocado pear seed extract were added to the $AgNO_3$ solution. The combination was subjected to incubation at ambient temperature until the yellow hue of the solution transitioned to a deep brown shade. The samples were centrifuged for 20 minutes at 5000 revolutions per minute, and the supernatant was disposed of after the process. A volume of 5 mL of deionised water was introduced to the precipitate, followed by another round of centrifugation under identical conditions. The procedure was replicated. Subsequently, the ultimate precipitate was subjected to a temperature of 60˚C in a hot air oven for 30 minutes (Naveed *et al.*, 2022).

Preparation of Adsorbate

All compounds utilized in the studies were of analytical grade. To make a stock solution, 1000 mg of lead nitrate (Merck) was dissolved in one litre of distilled water. Additionally, 10 mL of strong Nitric acid was added to the solution to avoid hydrolysis. The stock solution underwent dilution to get various quantities of lead ions necessary for the tests (Dubey and Shiwani, 2011).

Characterization of Adsorbents

Fourier Transform InfraRed Spectroscopy (FTIR)

The Fourier Transform Infrared (FTIR) Spectrophotometer was employed to ascertain the functional groups present in the samples (Naveed *et al.*, 2022).

Scanning Electron Microscope (SEM) Analysis

SEM was employed to ascertain the structural characteristics of the nanoparticles acquired. The dried samples were affixed to a sample holder using double conductive tape at room temperature. A platinum-gold coating layer was administered to the samples to enhance conductivity. Subsequently, the samples were subjected to visualization using an 80 kV voltage (Naveed *et al.*,2022).

X-ray Diffraction (XRD) Analysis

X-ray diffraction (XRD) was employed to analyze the crystalline nature of the AgNPs. The experiment employed a powdered material, and the scanning mode was conducted using a current of 30 mA, a voltage of 40 kV, and Cu/Kα radiation. The

diffraction pattern was then recorded within the 2θ angle range of 20^0C–70^0C.

The Scherrer equation (1) was used to determine the particle size and is given by.

$$D = \frac{K\lambda}{\beta Cos\theta} \quad (1)$$

Where D is the nanocomposite crystalline size, K represents the Scherrer constant (0.98), ⋋ denotes the wavelength (1.54), β denotes the full width at half maximum (FWHM).

Batch Adsorption process

The batch experiments were performed using adsorbent material placed in Erlenmeyer flasks and sealed with glass stoppers to minimise evaporation. The mixtures were stirred using a mechanical, magnetic stirrer at 200 revolutions per minute. The objective was to determine the optimal conditions in terms of pH, adsorbent type, and lead(II) ion concentrations.

Effect of pH

To determine the effect of pH on the adsorption of lead(II) ions onto Avocado pear silver nanoparticles, the adsorption mixture was brought into equilibrium with a 20 ml solution containing 150 mg/dm^{-3} of lead(II) ions and dried adsorbent. The experiment was conducted at pH levels 2, 4, 6, 8, and 10. The pH was adjusted using 0.1 M hydrochloric acid (HCl) and 0.1 M sodium hydroxide (NaOH) solutions. The experiment regulated the adsorbent quantity to 0.1g, the temperature to 30^0C, and the duration to 60 minutes.

Effect of adsorbent dosage

The impact of the adsorbent dose was investigated by manipulating the weights of the Nanocomposites within the range of 0.1g, 0.2g, 0.3g, 0.4g, and 0.5g. Subsequently, these samples were subjected to testing under the specified experimental circumstances. The experimental conditions included a time duration of 60 minutes, a temperature of 300°C, a pH value of 6, and a concentration of 150 mg/L.

Effect of time

The study investigated the impact of time by manipulating the duration at intervals of 30 minutes, namely at 30, 60, 90, 120, 150, and 180 minutes. These variations were examined under the specified experimental settings. The experimental conditions included a temperature of 300°C, a pH value of 6, a dosage of 0.1g, and a 150 mg/L concentration.

Effect of Temperature

The study investigated the impact of temperature by manipulating the duration at intervals of 5°C, namely at 30, 35, 40, 45 and 50°C. These variations were examined under the specified experimental settings. The experimental conditions included a pH value of 6, a dosage of 0.1g, and a concentration of 150 mg/L.

Effect of initial metal ion concentration

The impact of the initial metal ion concentration was investigated by manipulating concentrations at 100 mg/L, 150 mg/L, 200 mg/L, 250 mg/L, and 300 mg/L under the specified experimental settings. The experimental conditions included a time duration of 60 minutes, a dosage of 0.1g, a temperature of 300°C, and a pH level of 6. The concentrations of the metal solutions were determined using

atomic absorption spectroscopy, specifically, the AA500F atomic absorption spectrophotometer. A control experiment was also conducted utilising identical solutions and equipment, except for the nano-composite adsorbents.

Adsorption Capacity

The experimental adsorption capacity (qe mg/g) after equilibrium was calculated as follows:

$$q_{e=(C_0-C_e)\frac{V}{m}} \quad (2)$$

Co and Ce are Pb's initial and equilibrium concentrations (mg/L). "V" is the volume of the solution, and "m" is the amount of adsorbent.

$$E\% = \frac{(C_0-C_e)}{C_0} x\ 100 \quad (3)$$

Where E is the absorption capacity.

Kinetics Studies

The kinetic investigation was conducted using various concentrations (10mg L^{-1}, 20mg L^{-1}, 30mg L^{-1}) of solutions at ambient temperature (300K) in contact with the nanoparticle (adsorbent) generated at the optimal dose. Samples of lead (II) solutions were collected at intervals ranging from 20 to 100 minutes, and the metal concentration was determined. The calculation of metal uptake was performed utilizing kinetic equations. Analyzing the sorption kinetic data for Pb(II) on the adsorbent involved using pseudo-first-order and pseudo-second-order sorption equations.

Equilibrium Isotherm Models

Two models, the Langmuir and Freundlich isotherms, were employed in the investigation of the adsorption isotherm. Based on experimental data, isotherm plots were generated to illustrate the relationship between the quantity of Pb(II) adsorbed per unit mass (mg/g) and the equilibrium solution concentration during the adsorption process of Pb(II).

Thermodynamic studies

Thermodynamic equations were employed to determine adsorption's spontaneity and investigate the impact of temperature on the adsorption process. Equation 5 is used to calculate the equilibrium constant, Kc. Consequently, the thermodynamic equation, known as the Van't Hoff isotherm equation, can be expressed linearly, as depicted in equation 4.

$$\Delta G = -RTlnk_C \quad (4)$$

$$lnk_C = \left(\frac{C_A}{C_e}\right) \quad (5)$$

$$lnk_C = \left(\frac{-\Delta H}{R}\right).\frac{1}{T} + \left(\frac{\Delta S}{R}\right) \quad (6)$$

The symbols Kc and T(K) represent the adsorption equilibrium constant and temperature, respectively. The equilibrium concentrations in the solid and solution phases are CA (mg/g) and Ce (mg/L), respectively. The standard enthalpy, entropy, and Gibbs energy, represented by ΔH (kJ/mol), ΔS (kJ/mol K), and ΔG (kJ/mol), respectively, are defined. The Van't Hoff equation was employed to get the values of ΔH, ΔS, and ΔG.

RESULTS AND DISCUSSION

The Fourier Transform Infrared (FTIR) spectra of APS and AgAPS

This study focuses on the infrared spectroscopic analysis of avocado pear seed (APS) and the synthesized silver nano-particle avocado pear seed (AgAPS). Figures 1 and 2 depict the Fourier Transform Infrared (FTIR) spectra of APS and AgAPS, respectively. The signals that were observed are displayed in Table 1.

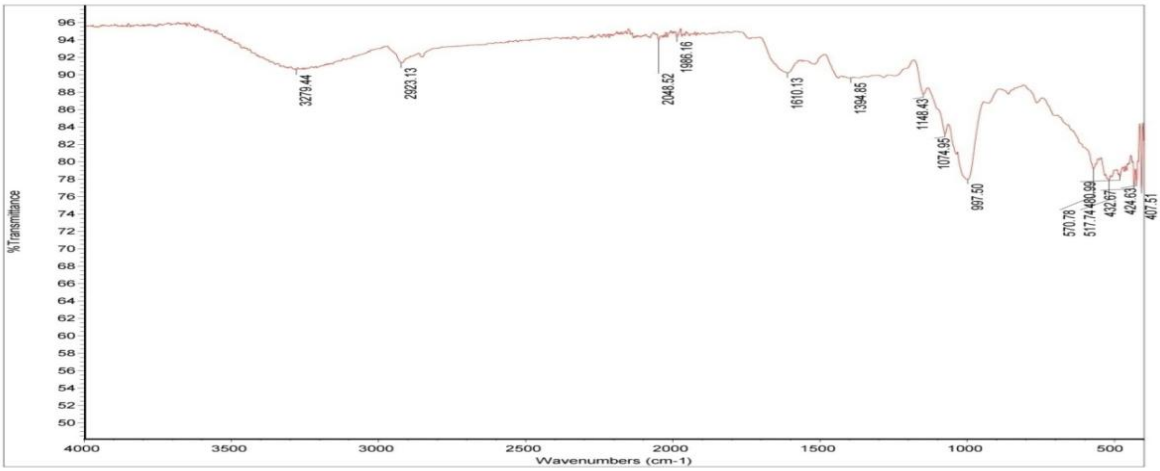

Figure 1: Infrared Spectroscopic Spectrum for avocado pear seed (APS)

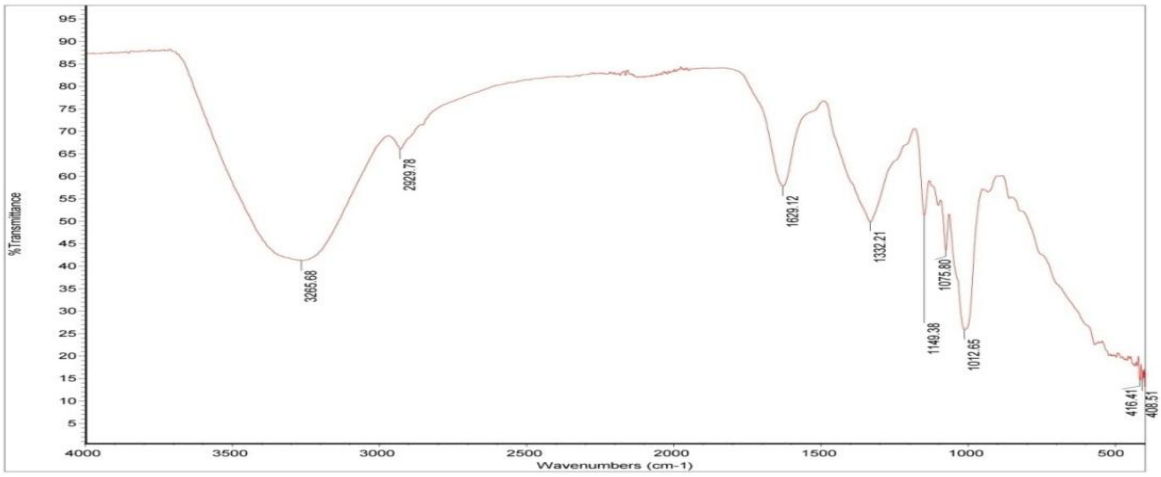

Figure 2: Infrared Spectroscopic Spectrum of Silver Oxide nano-particle-Avocado Pear Seed (AgAPS)

Table 1: Assignments of the IR spectra bands of functional groups in APS and AgAPS

APS band positions (cm^{-1})	AgAPS band positions (cm^{-1})	Proposed signal group

3279	3265	OH stretching
2923	2929	CH stretching
2048 and 1986	-	C≡C of alkynes
1610	1629	C=O stretching
1394	1332	C-H bending
1148	1149	C-O stretching
1074	1076	C-O stretching

The absorption band observed at 3279 cm^{-1} in the APS sorbent spectrum can be attributed to the presence of the hydroxyl (OH) functional group. Similarly, the band observed at 2923 cm^{-1} can be attributed to the stretching vibrations of the carbon-hydrogen (CH) bonds. The absorptions occurring at wavenumbers of 2048 cm^{-1} and 1986 cm^{-1} can be attributed to the presence of C≡C functionality in alkynes. Additionally, the stretching of the C=O bond in carbonyl compounds was seen at a wavenumber of 1610 cm^{-1}. Furthermore, CH bending was detected at a wavenumber of 1394 cm^{-1}, whilst C-O stretching vibrations were identified at 1148 cm^{-1} and 1074 cm^{-1}. Following the deposition of silver oxide nanoparticles (AgNOPs) over APS, notable alterations were detected in the absorption spectra of various functional groups. Specifically, the OH group exhibited a shift from 3279 to 3265 cm^{-1}, the C-H bands saw a shift from 2923 to 2929 cm^{-1}, the C=O bands displayed a change from 1610 to 1629 cm^{-1}, and the C≡C bands were reported to vanish entirely. This observation demonstrates the interaction between the impregnated silver nanoparticles (AgONPs) and the functional groups in the avocado pear seed (APS). Furthermore, the existence of surface functional groups on both the APS and AgAPS sorbents suggests the capability of these produced sorbents to eliminate contaminants from aqueous solutions. This statement aligns with Akpomie & Conradie's (2020b) findings.

XRD Characterization

XRD Spectroscopic Studies for avocado pear seed (APS) and Silver Oxide nano-particle-avocado Pear Seed (AgAPS)

The X-ray diffraction (XRD) spectra depicted in Figure 3 offer insights into the crystal phase of the Sorbents. In the case of APS, the diffraction peaks observed at 2θ values of 15^0, 17^0 and 27^0 indicate the characteristic cellulose diffraction pattern associated with agro-waste, as reported by Dai *et al.,* (2020). The confirmation of the face-centred cubic structure of Ag nanocomposites in AgAPS, as depicted in Figure 4, was achieved through the analysis of 2θ diffractions. Specifically, diffraction peaks were observed at 38^0, 44^0, 65^0, and 78^0, corresponding to the (111), (200), (220), and (311) Ag reflections, respectively. This observation provides evidence of comparable nanomaterials within the AgAPS composites.

The study conducted by He *et al.,* (2017) found comparable diffraction patterns for silver nanoparticles that were synthesized using the seed extract of Alpinia Katsumodai Hayata (AKH).

Figure 4 employs the Scherrer equation to determine the particle size of the higher peaks in the spectra. The 2θ diffractions at the 5 highest peaks, 150, 170, 390, 650, and 780, have an average particle size of 95nm.

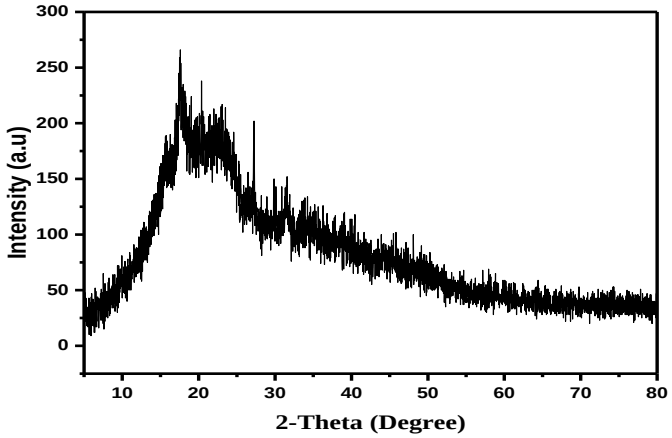

Figure 3: XRD Spectroscopic Spectrum for avocado pear seed (APS)

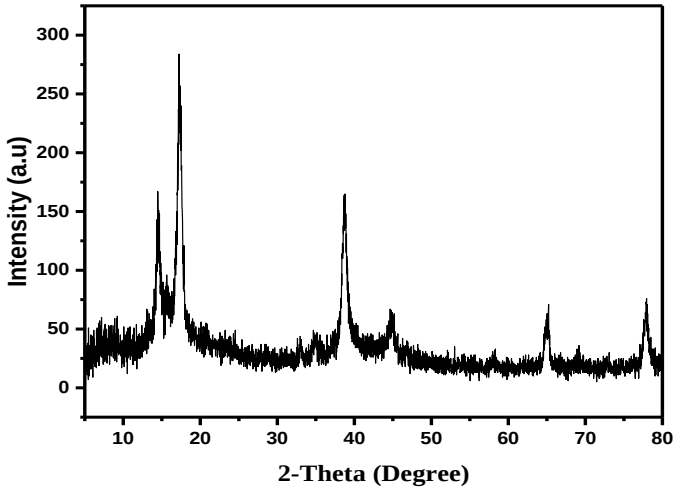

Figure 4: XRD Spectroscopic Spectrum for Silver Oxide nano-particle-Avocado Pear Seed (AgAPS)

SEM Characterization

Various magnifications of Scanning Electron Microscopy (SEM) were employed to examine the surface morphology of the synthesized silver oxide nanocomposites, as illustrated in Figures 5-8. Figures 5-6 analysis reveals that the avocado pear seed

nanocomposite (AgAPS) exhibits comparable rough surfaces, an irregular surface structure, and a hexagonal shape. In contrast, images 7-8 depict the avocado pear biomass with a sparse distribution and a distinct lack of the diagonal shape observed in AgAPS. The photographs depict the development of an uneven surface structure in the form of silver oxide composite agglomerates. Zinc oxide nanoparticles from *Costus Afers* leaf extract produced similar spectra (Chukwuemeka-Okoye *et al.*, 2023).

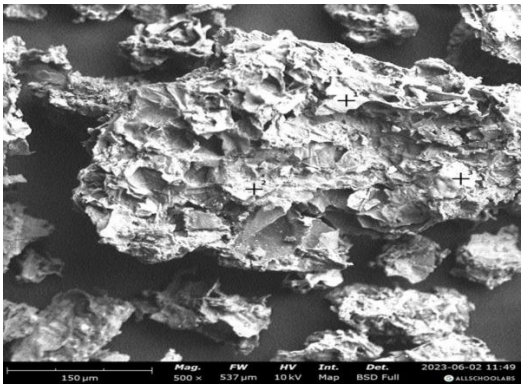

Figure 5: SEM **Spectrum of 500 Magnification for Silver Oxide nano-particle-Avocado Pear Seed (AgAPS**

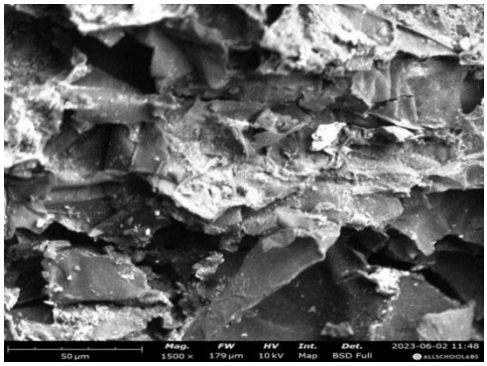

Figure 6: SEM **Spectrum of 1500 Magnification for Silver Oxide nano-particle-Avocado Pear Seed (AgAPS)**

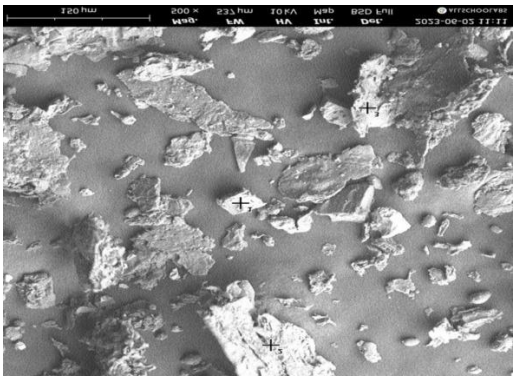

Figure 7: SEM **Spectrum of 500 Magnification for raw Avocado Pear Seed (APS)**

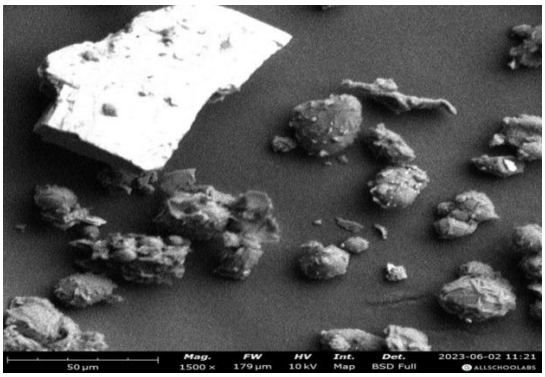

Figure 8: SEM **Spectrum of 1500 Magnification for raw Avocado Pear Seed (APS)**

Adsorption studies of Lead unto Avocado Pear Seed

Effect of pH on the adsorption of lead onto avocado pear seed

In any adsorption investigation, the adsorbent and adsorbate species are impacted by the pH of the wastewater solution. This results in changes to the surface charge and speciation at different pH levels due to the protonation or deprotonation of the functional groups in both the adsorbent and the adsorbate (Akpomie & Conradie, 2020). During the adsorption process, charged species may come into contact with one another via electrostatic interactions. As a result, solution pH is a crucial factor that influences adsorption and should be considered. Figure 9 displays the findings of the impact of pH on lead adsorption onto APS and AgAPS. The sorption capacity reached its highest at pH 6 (27.2225 mg/g) for AgAPS and pH 8 (23.7568 mg/g) for APS. The equilibrium sorption capacity was lowest for APS at pH 4 (15.6108 and 17.0811 mg/g), respectively. The decreased sorption capacity at low pH can be explained by the possibility that H^+ ions may compete with Pb^{2+} ions for the adsorbent's adsorption sites at an acidic pH, preventing lead ions from adhering to the surface—other reports of comparable outcomes are available (Hameed & El-Khaiary, 2018).

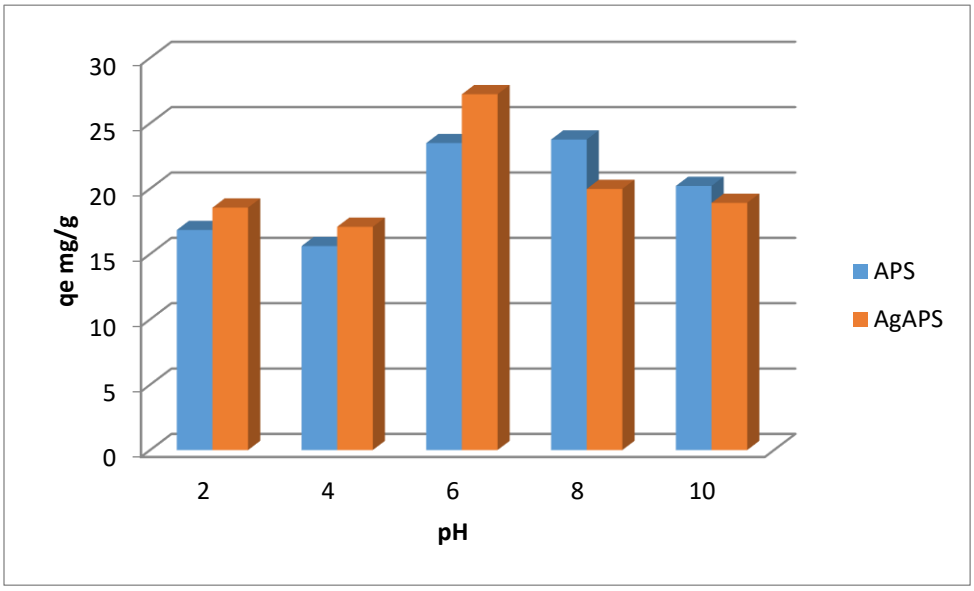

Figure 9: Effects of pH of the adsorption of lead onto avocado pear seed

Effect of Dosage on the Adsorption of Avocado Pear Seed

The dosage of the adsorbent is a significant and crucial parameter that has a notable impact on the adsorption process. Figure 10a displays the outcomes of the influence of adsorbent dosage on the adsorption process of lead onto APS and AgAPS. An increase in the adsorbent dose from 0.1g to 0.5g resulted in a percentage removal increase ranging from 78.2869% to 80.3505% for AgAPS and from 89.8527% to 93.0206% for APS. The observed phenomenon can be ascribed to an augmentation in surface area and active adsorption sites. However, a contrasting pattern was identified, as depicted in Figure 10b, wherein a decline in adsorption capacity was found with an increase in adsorbent dosage. The potential cause of this phenomenon could be attributed to a reduction in the overall surface area accessible for lead to bind, which may arise from the overlapping or aggregation of adsorption sites (Dawodu & Akpomie, 2014). Consequently, with an increase in the adsorption dosage, there was a corresponding drop in the lead adsorbed per unit mass, which reduced the overall adsorption capacity. Nevertheless, the maximal adsorption capacity can be determined using column tests by employing an excessive quantity of adsorbate (Zafar *et al.*, 2006).

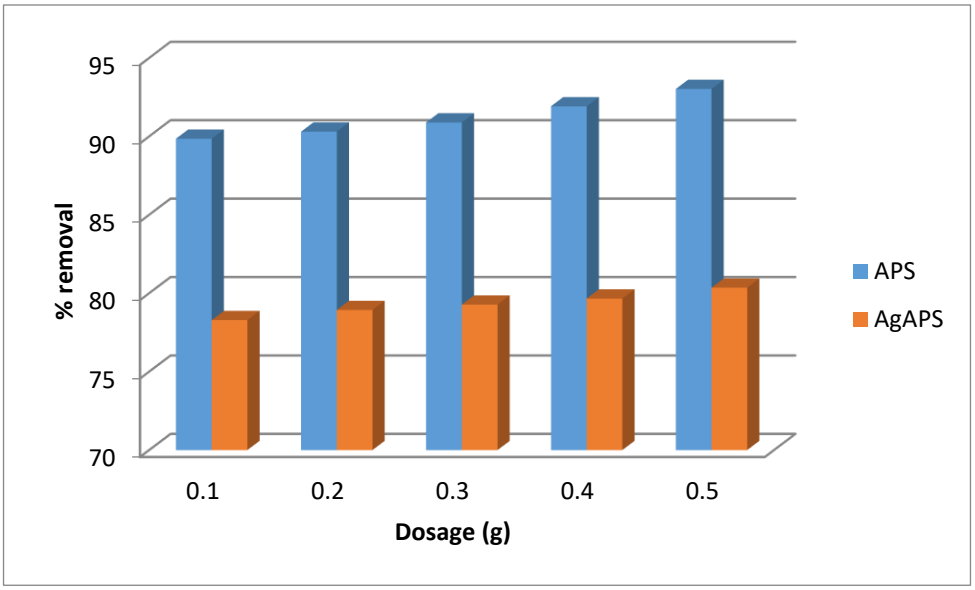

Figure 10a: Effect of Dosage on the Adsorption of Avocado Pear Seed (Percentage removal)

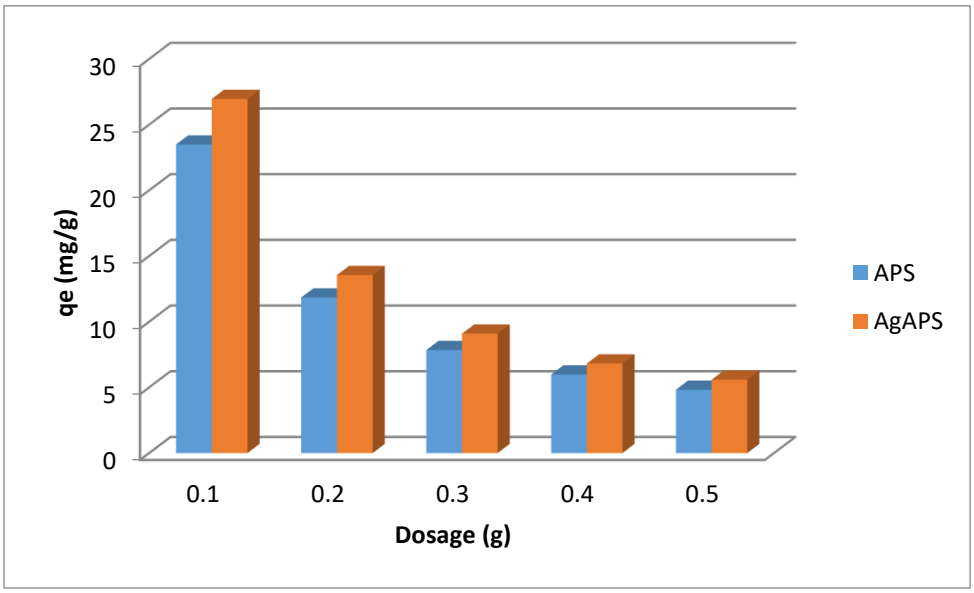

Figure 10b: Effect of Dosage on the Adsorption of Avocado Pear Seed

Effects of time on the adsorption of lead onto raw avocado pear seed

The findings about the influence of time on the adsorption process of avocado pear seed are illustrated in Figure 11. As anticipated, the proportion of lead removed exhibited an upward trend as the duration of sorption extended from 30 minutes to 180 minutes. A duration of 180 minutes yielded a peak adsorption capacity of 27.9 mg/g for the AgAPS and 23.9 mg/g for the APS. The rapid initial adsorption seen in this study may be attributed to the initial adsorption onto the material's surface, followed by penetration into its interior microscopic spaces (Dawodu & Akpomie, 2014).

The decrease in adsorption rate over time can be attributed to a process controlled by attachment, which is produced by a reduced number of sites for active adsorption (Nwadiogbu *et al*., 2016). The findings demonstrated the efficient and consistent characteristics of the process, as only a negligible disparity was in the initial and final contact time duration. Throughout the study, it was seen that AgAPS exhibited an excellent adsorption capability compared to APS. The possible cause for this phenomenon could be the augmentation of active adsorption sites resulting from the introduction of Ag molecules. The findings obtained in this investigation are consistent with the reports of Akpomie & Conradie (2020).

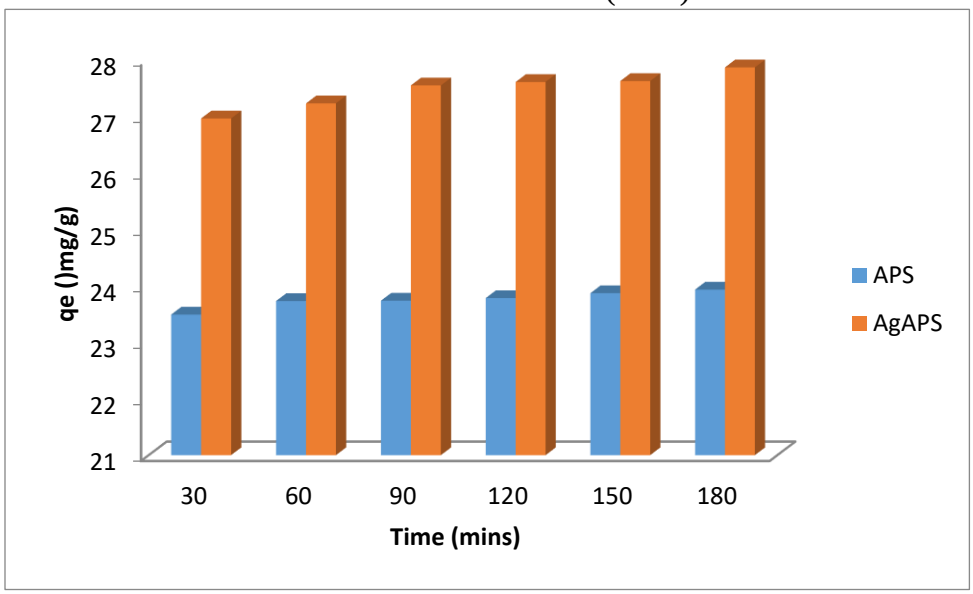

Figure 11: Effects of time on the adsorption of lead onto raw avocado pear seed

The temperature of wastewater is a significant determinant in the absorption of various contaminants from the solution. The present study investigated the impact of temperature on the adsorption behaviour of lead onto APS and AgAPS, as illustrated in Figure 12. The temperature was raised from 30^0 to 50^0 C, resulting in an elevation in the removal of lead ions. Specifically, the removal increased from 23.4860 mg/g to 25.0496 mg/g for APS, while AgAPS went from 26.9558 mg/g to 28.1573 mg/g. According to Akpomie & Conradie (2020), it can be inferred that elevated temperatures

promote the adsorption of lead ions onto both adsorbents. Additionally, the authors suggest that the reaction process has an endothermic nature. The enhanced adsorption capacity observed may be attributed to the increased mobility of lead molecules at higher temperatures, facilitating more significant contact with the active sites of the adsorbent (Akpomie & Conradie, 2020b). The increase in temperature is also associated with generating novel active sites on the surface of the adsorbent due to eliminating certain impurities on the surface (Akpomie & Conradie, 2020b). Nevertheless, a marginal decline in the adsorption capacity was seen at a temperature of 50^0C for both materials.

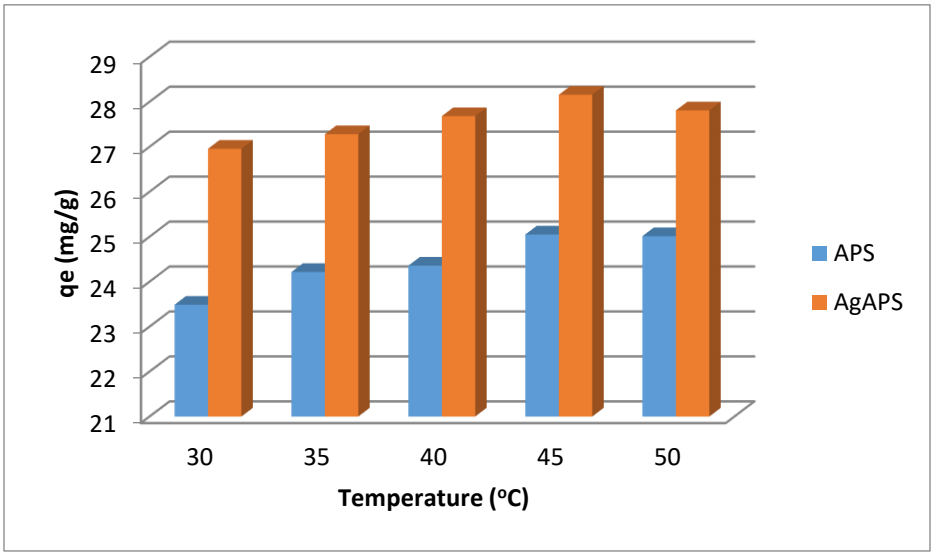

Figure 12: Effect of temperature on the adsorption of lead onto avocado pear seed

Effect of Concentration on the adsorption of lead onto avocado pear seed shell

The findings about the impact of concentration on lead adsorption onto APS and AgAPS are illustrated in Figure 13. An increase in the concentration of the initial metal ion from 100mg/L to 300mg/L corresponded with an increase in the adsorption capacity of the metal ion. This can be attributed primarily to the higher quantity of metal ions in the solution, leading to an elevated collision rate and, consequently, more effective collisions. However, an inverse relationship was detected between the percentage removal and the initial metal ion concentration, indicating a decrease as the concentration increased. The adsorbent surface possesses a finite quantity of active adsorption sites. Since the biomass adsorbent dosage employed remained constant at 0.1g throughout the shifting concentration of 100-300mg/L. hence, the proportion of lead ion per adsorbent is low at the beginning metal ion concentration. As the initial metal ion concentration increases, the metal ion/adsorbent ratio shows a noticeable upward trend. Consequently, this intensifies the competition among metal ions for the limited active sites on the adsorbent material, decreasing the percentage of metal ion removal. Additionally, the observed pattern can be ascribed to the growing impediment caused by mass transfer resistance, which is a consequence of the escalating solution viscosity accompanying the rise in metal ion concentration (Prajapeti *et al*., 2020).

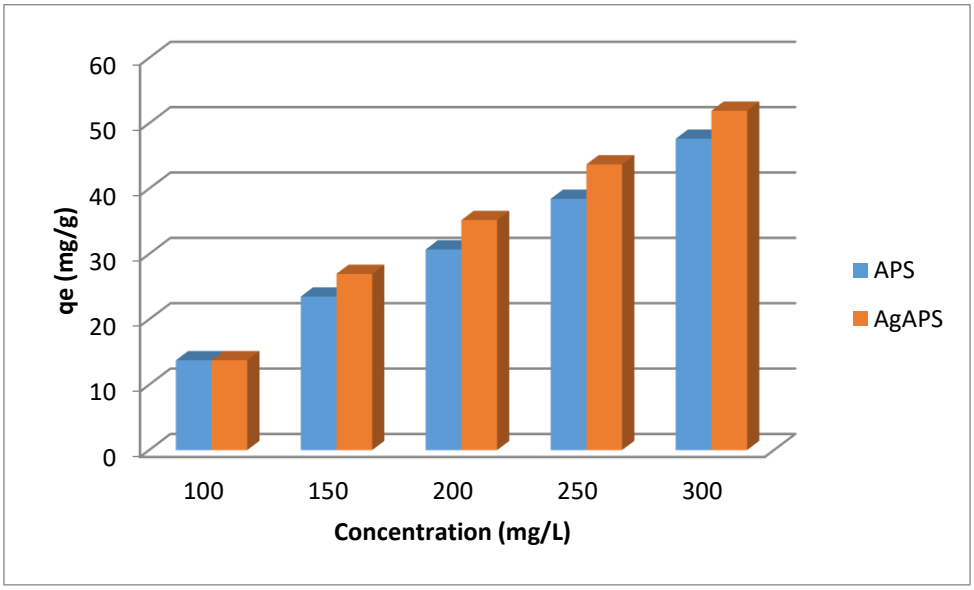

Figure 13: Effect of Concentration on the adsorption of lead onto avocado pear seed

Kinetic Studies

To elucidate the process of lead adsorption onto APS and AgAPS, the experimental data were analysed using the pseudo-first-order kinetic, pseudo-second-order, and intra-particle diffusion kinetic models. Plots illustrating the pseudo-first-order and pseudo-second-order kinetic models are depicted in Figures 14 and 15, respectively. The coefficient of determination R^2 values for the pseudo-second-order model (0.999 and 1.000) exhibit higher magnitudes than the pseudo-first-order model (0.913 and 0.898) for AgAPS and APS, respectively. Additionally, the estimated qe values obtained from the pseudo-second-order model demonstrate closer proximity to the experimental values than the pseudo-first-order model. According to Akpomie & Conradie (2020), the adequacy of fit and the accuracy of prediction for qe both suggest that the pseudo-second-order model offers a more comprehensive depiction of the adsorption mechanism of lead onto APS and AgAPS. Furthermore, chemisorption is likely the underlying mechanism of attraction. Hameed & Khaiary (2008) achieved a comparable outcome in the adsorption process of malachite green onto rattan sawdust.

The transportation of lead and other metal ions in solution from the aqueous phase to the adsorbent's surface and their diffusion into the porous particles' interior has been observed (Nwadiogbu *et al.*, 2016). According to Hill *et al.*, (1998) and Igwe & Abia (2006), a linear relationship between the quantity of adsorbate (qe) and the square root of time ($t_{1/2}$) is anticipated when the biosorption process involves intraparticle diffusion. Furthermore, if the line passes through the origin, it suggests that

intraparticle diffusion is the dominant mechanism controlling the process. In the scenario where the plots do not intersect at the origin, it has been postulated that the sorption process involves mechanisms beyond intra-particle diffusion, potentially indicating the presence of boundary layer control to some extent. The obtained intercept values of 26.41 and 23.26 for AgAPS and APS were recorded and displayed in Figure 16. In the context of the intra-particle diffusion model, it is suggested that the process of lead adsorption onto APS and AgAPS involves both surface reaction and diffusion into the porous structure of these materials. This finding aligns with previous studies conducted by Nwadiogbu *et al.*, (2014) and Akpomie & Conradie (2020).

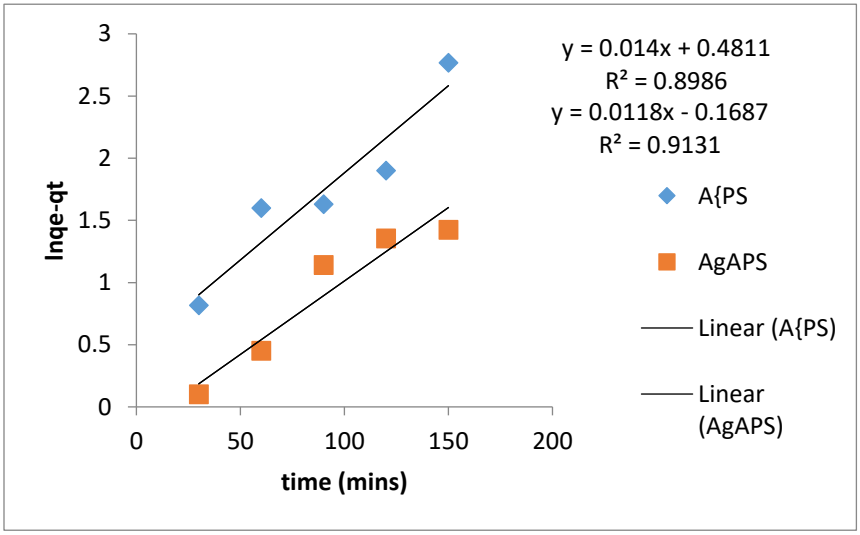

Figure 14: Pseudo first order kinetic plots for the adsorption of lead onto AgAPS and APS

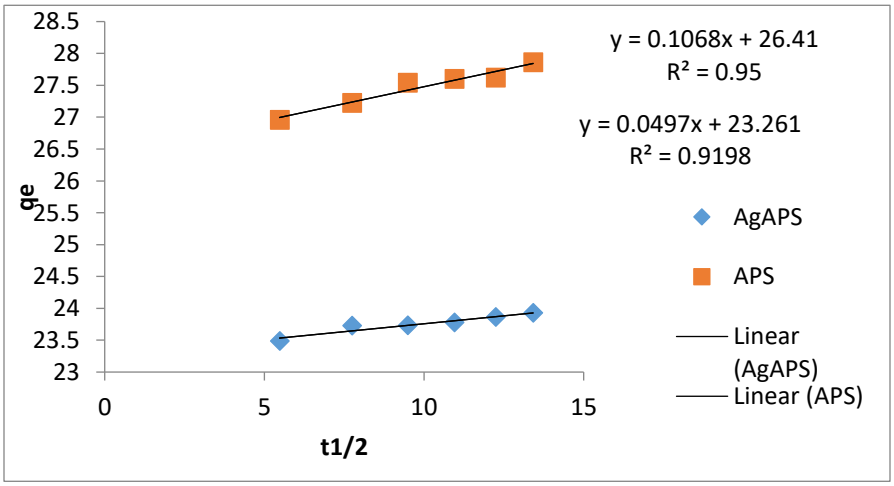

Figure 15: Pseudo second-order kinetic plot for the adsorption of lead onto AgAPS and APS

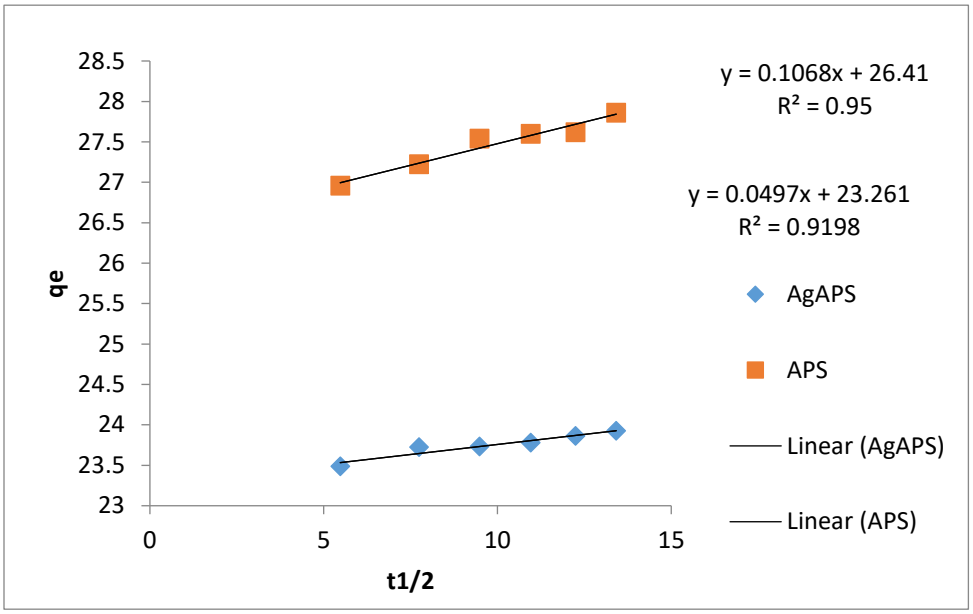

Figure 16: Intra-particle diffusion kinetic model for the adsorption of lead onto AgAPS and APS

Thermodynamics analysis of the adsorption of lead onto avocado pear seed

The thermodynamic parameters ΔHo, ΔSo, and ΔGo offer valuable insights into the heat changes, spontaneity, and randomness associated with the sorption process. Figure 17 displays a plot of the natural logarithm of the equilibrium constant (link) as a function of temperature. The corresponding thermodynamic parameters for the sorption of lead onto APS and AgAPS are presented in Table 2.

Table 2: Thermodynamic parameters for the sorption of lead onto avocado pear seed

	APS	AgAPS
ΔH (KJ/mol)	0.12471	8.314 x 10-3
ΔS (J/K)	50.973	13.427
Δ G 303K	-4342.50	-5494.25
ΔG 308K	-3362.47	-5615.64
ΔG 313K	-3432.15	-5744.54
ΔG 318K	-3475.34	-5881.51
ΔG 323K	-3612.97	-5940.70
R^2	0.441	0.766

The observed positive values of ΔHo for both APS and AgAPS suggest that the lead removal process by APS and AgAPS is endothermic. This finding implies that the adsorption of lead increases as the temperature rises. According to Somayeh *et al*., (2019), the positive value of ΔS^o indicates an increase in entropy at the solid-solution interface during the adsorption process and the subsequent development of structural changes. This suggests that the process is irreversible. In the opinion of Somayeh *et al.*, (2019), the presence of negative values in the Gibbs free energy indicates the spontaneous nature of the process. The increase in temperature leads to an elevation in the standard Gibbs free energy change (ΔG^o) in the system, resulting in a greater extent of adsorption. At higher temperatures, the metal ion undergoes hydration more rapidly, leading to an increase in its adsorption.

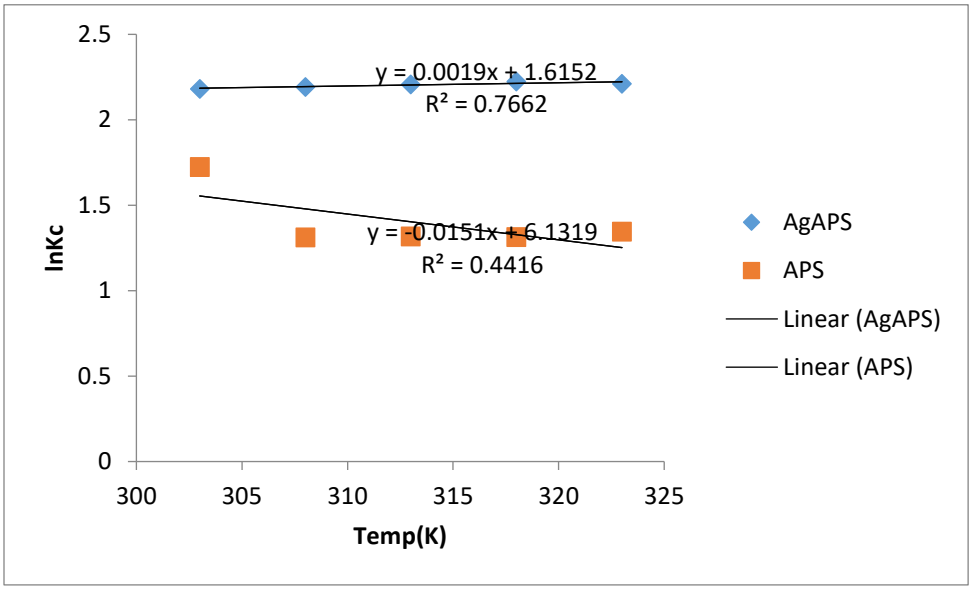

Figure 17: Thermodynamic plots for the adsorption of lead onto avocado pear seed

Equilibrium studies for lead sorption onto avocado pear seed

The sorption isotherm describes the correlation between the quantity of adsorbent extracted from the liquid phase and the mass of the adsorbent per unit at a consistent temperature (Nwadiogbu *et al.,* 2016). Additionally, the study conducted by Goes *et al*., (2020) offers valuable insights into the correlation between pollutants present in a solution and their interaction with the sorbent material.

The figures presented in this study depict the plots of the Langmuir model, which were utilized to evaluate the isotherm of lead adsorption onto APS and AgAPS. Specifically, Figure 18 illustrates the Langmuir model plot for APS, while Figure 19 represents the Langmuir model plot for AgAPS. Furthermore, the figures also display the plots of the Freundlich model, which were employed to evaluate the isotherm of lead adsorption onto APS and AgAPS. Figure 20 showcases the Freundlich model plot for APS, whereas Figure 21 exhibits the Freundlich model plot for AgAPS. The

isotherm parameters that have been derived are displayed in Table 3.

Table 3: Summary of isotherm parameters for lead sorption onto avocado pear seed

Models	Parameters	APS	AgAPS
Langmuir	RL (L/g)	0.1823	0.1101
	q_o (g/g)	0.624	3.906
	B	0.0299	0.0539
	R^2	0.976	0.825
Freundlich			
	1/n	16.06	3.679
	K_F	1.0 x 1023	1230.28
	R^2	0.924	0.795

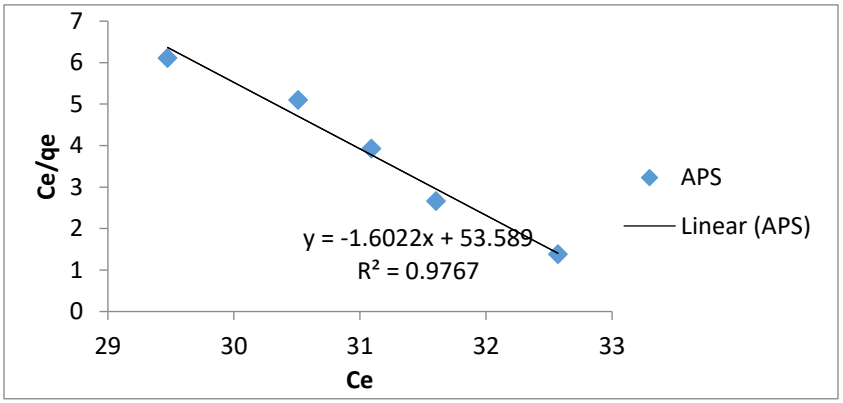

Figure 18: Langmuir isotherm plot for APS

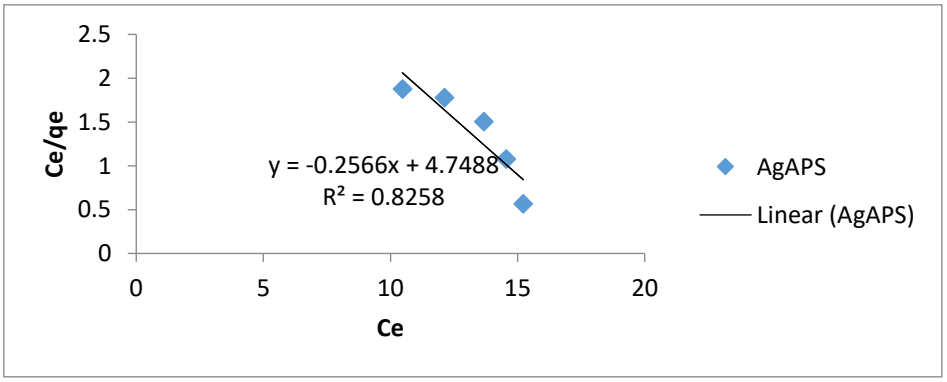

Figure 19: Langmuir isotherm plot for AgAPS

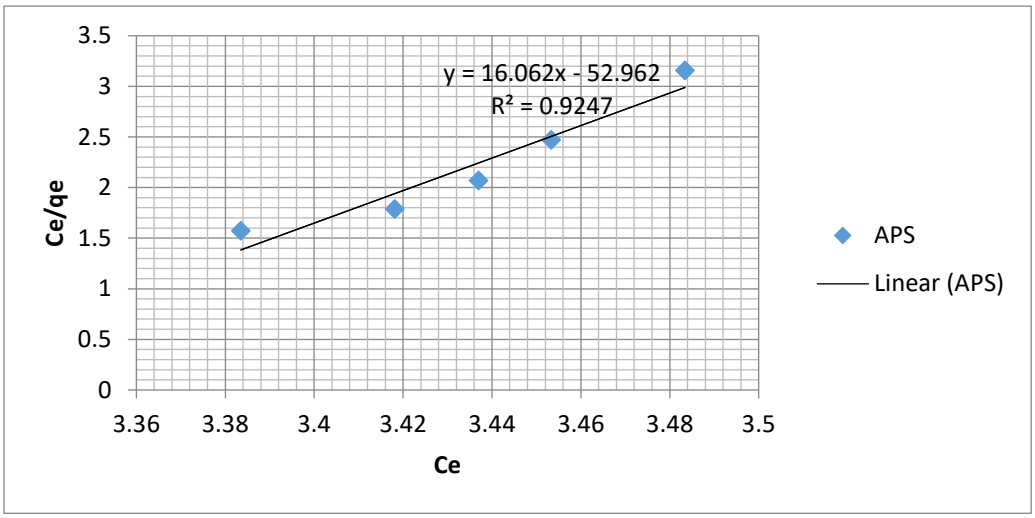

Figure 20: Freundlich isotherm plot for APS

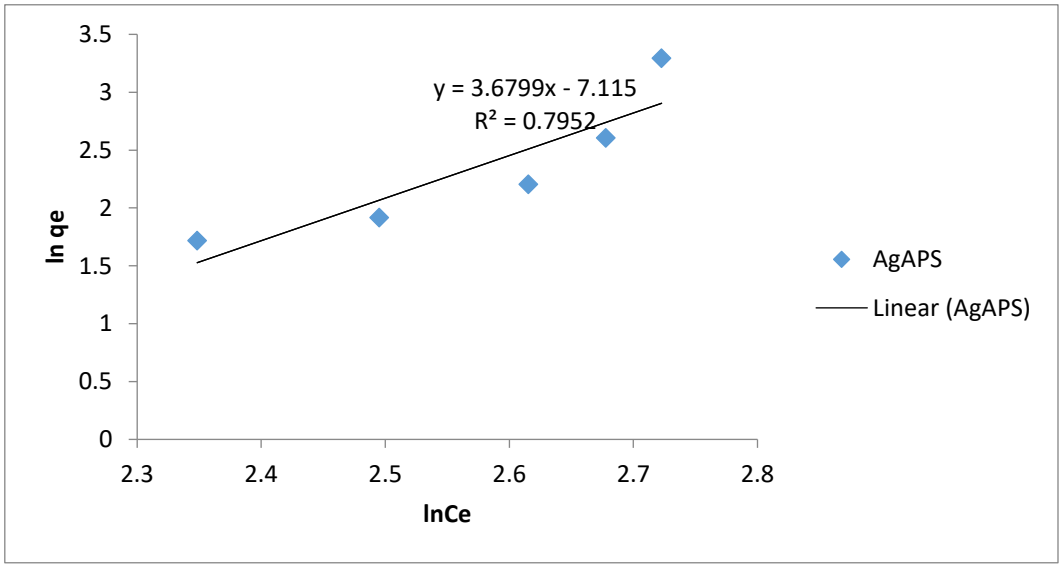

Figure 21: Freundlich isotherm plot for AgAPS

Based on the obtained R^2 values, it is evident that the Langmuir model exhibited the most favourable fit (R^2 0.976 and 0.825) for the APS and AgAPS samples, respectively. The suggestion is that the adsorption of lead onto APS and AgAPS is predicated on the formation of monolayer coverage. The fundamental characteristic of the Langmuir isotherm can be articulated to the non-dimensional constant, precisely the separation factor (RL). The adsorption process can be categorized into four types

based on the value of the separation factor (RL). These categories include irreversible adsorption (RL = 0), favourable adsorption (0 < RL < 1), linear adsorption (RL = 1), and unfavourable adsorption (RL > 1). The retention levels (0.1823 and 0.1101) obtained for APS and AgAPS in this study suggest favourable adsorption of lead.

CONCLUSION

The study shows the potential use of the nanocomposites from avocado peer seed in wastewater treatment. The XRD analysis has shown the synthesized materials' structural stability and nanoscale dimensions. The silver metal nanocomposites synthesized from avocado pear seeds exhibited adsorption capabilities towards lead ions in the simulated lead solution. The adsorption of lead ions by raw avocado pear seeds was higher when silver metal nanocomposite was present. The experimental findings indicate that the adsorbent exhibits greater adsorption capacity for nanocomposites compared to the untreated avocado pear seeds. The highest recorded percentage of lead removal was 80.35% for APS and 93.02% for AgAPS. In the study of lead adsorption kinetics, it was observed that the coefficient of determination R2 for the pseudo-second-order model was higher for AgAPS (0.99) and APS (1.00) compared to the pseudo-first-order model, which yielded values of 0.91 for AgAPS and 0.89 for APS. The observed intercept of the intra-particle diffusion model suggests that both surface reaction and diffusion into the porous structure of the materials govern the adsorption process. The adsorption behaviour of lead ions using APS and AgAPS adhered to the Langmuir isotherm.

RECOMMENDATIONS

This study reveals that the biosynthesized agro-waste nanocomposite from Avocado pear is environmentally friendly, less expensive, readily available, and non-toxic. It also demonstrates that it can be used as an effective adsorbent for the removal of lead ions from industrial wastewater.

Therefore, it is recommended that,

(i) To widen its application, it is necessary to carry out similar adsorption studies using this nanocomposite on other heavy metal ions to evaluate its efficiency on those heavy metal ions.

(ii) It would also be valuable if other agro wastes were employed in this study, improving the availability of the nanocomposite for industrial use.

(iii) More characterization analysis of the nanoparticle should be carried out in order to ascertain some intrinsic characteristics enhancing the adsorption.

REFERENCES

Akpome, K. G. and Conradie. J. (2020).Efficient synthesis of magnetic

nanoparticle-Musa acuminata peel composite for the adsorption of anionic dye. *Arab J. Chem.*, 13: 7115 – 7131.

Akpomie, K.G Panda Conradie, J. (2020b).Biogenic and chemically synthesized Solanum tuberosum peel-silver nanoparticle hybrid for the ultrasonic aided adsorption of bromophenol blue dye *Nature research*, 10: 17094.

Baran, M., Acay, H and Keskin, C. (2020). Determination of Antimicrobial and Toxic Metal Removal Activities of Plant-Based Synthesized (Capsicum annuum L. Leaves), Ecofriendly, Gold Nanomaterials. *Global Challenges*, 4. DOI: https://doi.org/10.1002 /gch2.201900104.

Božić, D., Gorgievski, M., Stanković, V., Cakic, M., Dimitrijević, S and Conić, V. (2021). Biosorption of lead ions from aqueous solutions by beech sawdust and wheat straw. Chemical Industry and Chemical Engineering Quarterly. DOI: https://doi.org/10.2298/ciceq191113021b.

Chowdhary, P., Bharagava, R. N., Mishra, S and Khan, N. (2020). Role of Industries in Water Scarcity and its Adverse Effects on Environment and Human Health. Environ. *Concerns Sustain. Dev.*, 235–256. DOI:10.1007/978-981-13-5889-0_12

Chukwuemeka-okorie, H.O., Ani, J.U., Agbo, S.U., Odewole, O.A., Ojo, F.K., Alum, O.L., Akpomie, K.G., Ofomatah, A.C and Aralu, C.C. (2023). Adsorptive performance of green synthesized zinc oxide nanoparticles for the removal of cadmium (II) and lead (II) ions. *IOP Conf. Series: Earth and Environmental Science*. 1178: 012021

Dawodu, F.A and Akpomie, K.G. (2014). Simultaneous adsorption of Ni(II) and Mn(II) ions from aqueous solution onto a Nigerian Kaolinite clay. *J. Mater. Res Technol.,* 3(2): 129-141.

Dai, H., Huang, Y., Zhary, H., Ma, L., Huary, H., Wu, J and Zhang, Y. (2020) Direct fabrication of hiearachially processed pineapple peal hydrogels for efficient conjured adsorption. *Carbohydrate polygon* 280, 115599

Das, P.A and Raj, K. (2023). Lead pollution: Impact on environment and human health and approach for a sustainable solution. *Environmental Chemistry and Ecotoxicology*, 5:79-85. DOI:https://doi.org /10.1016/j.enceco.2023.02.001

Denizil, A., Turkmen, D., Bakhshpour, M., Akgonullu, S and Asir, S. (2022). Heavy Metal Ions Removal from Wastewater Using Cryogels: A Review. *Front. Sustain., Sec.,* 3. DOI: https://doi.org/10.3389/frsus.2022. 765592

Djeussi, D. E., Noumedem, J. A. K., Mihasan, M., Kuiate, J. R and Kuete, V. (2020). Antioxidant Activities of Methanol Extracts of Thirteen Cameroonian Antibacterial Dietary Plants. *Journal of Chemistry*, 1–13. DOI:https://doi.org/ 10.1155/2020/8886762

Dubey, A and Shiwani, S. (2011). Adsorption of lead using a new green material obtained from Portulaca plant. *International Journal of Environmental Science and Technology*, 9(1): 15–20. DOI:https://doi.org/10.1007/s13762-011-0012-8

Fagbayigbo, B., Opeolu, B and Fatoki, O. (2020). Adsorption of perfluorooctanoic acid (PFOA) and perfluorooctane sulfonate (PFOS) from water using leaf biomass (*Vitis vinifera*) in a fixed-bed column study. *Journal of Environmental Health Science*

and Engineering, 18, 221 - 233. https://doi.org/10.1007/s40201-020-00456-1.

Fanourakis, S. K., Peña-Bahamonde, J., Bandara, P. C and Rodrigues, D. F. (2020). Nano-based adsorbent and photocatalyst use for pharmaceutical contaminant removal during indirect potable water reuse. *Npj Clean Water,3*(1). DOI:https://doi.org/10.1038/s41545-019-0048-8

Guo, G., Zhang, D and Wang, Y. (2020). Characteristics of heavy metals in size-fractionated atmospheric particulate matters and associated health risk assessment based on the respiratory deposition. *Environmental Geochemistry and Health*, 43, 285-299. DOI:https://doi.org/10.1007/s10653-020-00706-z.

Hameed, B. H and El-khaiary, M.I. (2008). Malaite green adsoption by raw rathan dust, Isotherm, Kinetic and mechanism. *Journal of hazardous materials*, 159: 574 – 579.

He, Y, Wei, F, Ma, Z., Zhang, I., Yang, Q., YaO, B., Huang, Z., Li, J., Zeng, C and Zhang, Q. (2017). Green Synthesis of Silver nanoparticles using seed extract of Alpinia Katsumadai and their antioxidant, Cytotoxicity and anti-bacterial activities. *RSC Adv.*, 7: 39642 – 39851.

Hill, C.A.S., Jones, D., Strickland, G and Cetin, N.S. (1998). Kinetic and mechanistic aspects of the acetylation of wood with acetic anlydride.*Holzforschung*, 52: 623 – 629.

Igwe, J. C and Abia A.A. (2006). A bio separation process for remaining heavy metals from waste water using biosorbents. *African journal of Biotechnology*, 5: 1167 – 1179.

Karthikeyan, S., Arumugam, S., Muthumanickam, J., Kulandaisamy, P., Subramanian, M., Annadurai, R., Senapathi, V and Sekar, S. (2021). Causes of heavy metal contamination in groundwater of Tuticorin industrial block, Tamil Nadu, India. *Environmental Science and Pollution Research*, 1-16. DOI:https://doi.org/10.1007/s11356-020-11704-0.

Khan, F., Pandey, P., Agarwal, S and Singh, M. (2023).Nano Adsorbents in Wastewater Treatment: A New Paradigm in Wastewater Management. *Letters in Applied NanoBioScience*, 12(4):1-17. Doi: https://doi.org/10.33263/LIANBS124.125

Khan, F., Shariq, M., Asif, M., Siddiqui, M., Malan, P and Ahmad, F. (2022). Green Nanotechnology: Plant-Mediated Nanoparticle Synthesis and Application. *Nanomaterials*, 12. DOI:https://doi.org/10.3390/nano12040673.

Landrigan, P. J., Fuller, R., Acosta, N. J. R., Adeyi, O., Arnold, R., Basu, N. N., Baldé, A. B., Bertollini, R., Bose-O'Reilly, S., Boufford, J. I., Breysse, P. N., Chiles, T., Mahidol, C., Coll-Seck, A. M., Cropper, M. L., Fobil, J., Fuster, V., Greenstone, M., Haines, A., Hanrahan, D., Hunter, D., Khare, M., Krupnick, A., Lanphear, B., Lohani, B., Martin, K., Mathiasen, K.V., McTeer, M.A., Murray, C.J.L., Ndahimananjara, J.D., Perera, F., Potočnik, J., Preker, A.S., Ramesh, J., Rockström,J., Salinas, C., Samson, L.D., Sandilya, K., Sly, P.D., Smith, K.S.,Steiner, A., Stewart, R.B., Suk, W.A., van Schayck, O.C.P., Yadama, G.N., Yumkella, K and Zhong, M. (2018). The Lancet Commission on pollution and health. *The Lancet*, 391(10119), 462–512.

DOI:https://doi.org/10.1016/s0140-6736(17)32345-0

Landrigan, P. J., Fuller, R., Fisher, S., Suk, W. A., Sly, P., Chiles, T. C and Bose-O'Reilly, S. (2019). Pollution and Children's Health. *Sci. Total Environ.,* 650 (2): 2389–2394. DOI:10.1016/j.scitotenv.2018.09.375

Li, M., Li, Y., Zhang, X., Zheng, H., Zhang, A., Chen, T., Liu, W., Yu, Y., Liu, J., Du, Q., Wang, D and Xia, Y. (2020). One-step generation of S and N co-doped reduced graphene oxide for high-efficiency adsorption towards methylene blue. *RSC Advances*, 10:37757 - 37765. DOI: https://doi.org/10.1039/d0ra06296k.

Naveed, M., Bukhari, B., Aziz, T., Zaib, S., Mansoor, M. A., Khan, A. A., Shahzad, M., Dablool, A. S., Alruways, M. W., Almalki, A. A., Alamri, A. S and Alhomrani, M. (2022). Green Synthesis of Silver Nanoparticles Using the Plant Extract of Acer oblongifolium and Study of Its Antibacterial and Antiproliferative Activity via Mathematical Approaches. *Molecules*, 27(13), 4226. DOI:https://doi.org /10.3390/molecules27134226

Nwadiogbu, J. O., Okoye, P.A.C., Ajiwe, V.I.E and Nnaji, J.N. (2016). Removal of crude oil from aqueous medium by sorption on hydrophobic corncobs: Equilibrium and kinetic studies. *Journal of Taibah University for science*, 10(1):56-63.

Patel, H. (2021). Comparison of batch and fixed bed column adsorption: a critical review. *International Journal of Environmental Science and Technology*, 19:10409-10426. DOI: https://doi.org/ 10.1007/s13762-021-03492-y.

Prajapeti, A.K., Das, S. and Mondal, M.K. (2020).Exhaustive studies on toxic Cr(VI) removal mechanism from aqueous solution using activated carbon of Aloe vera waste leaves. *Journal of Molecular Liquids*,307:112956. DOI:10.1016/j.molliq.2020.112956

Sadegh, H., Ali, G. A. M., Gupta, V. K., Makhlouf, A. S. H., Shahryari-ghoshekandi, R., Nadagouda, M. N., Sillanpaa, M and Megiel, E. (2017). The role of nanomaterials as effective adsorbents and their applications in wastewater treatment. *Journal of Nanostructure in Chemistry*, 7(1):1–14. DOI: https://doi.org/10.1007/s40097-017-0219-4

Sarkar, J., Mridha, D., Sarkar, J., Orasugh, J. T., Gangopadhyay, B., Chattopadhyay, D., Roychowdhury, T and Acharya, K. (2021). Synthesis of nanosilica from agricultural wastes and its multifaceted applications: A review. *Biocatalysis and Agricultural Biotechnology*, 37, 102175. DOI:https://doi.org/10.1016/j.bcab.2021.102175

Shaddick, G., Thomas, M., Mudu, P., Ruggeri, G and Gumy, S. (2020). Half the world's population are exposed to increasing air pollution. *npj Climate and Atmospheric Science*, 3: 1-5. DOI:https:// doi.org/10.1038/s41612-020-0124-2.

Singh, N.B., Nagpal, G.; Agrawal, S and Rachna. (2018). Water purification by using Adsorbents: A Review. *Environmental Technology and Innovation*, 11, 187-240. DOI:https://doi.org/10.1016/j.eti.2018.05.006.

Soliman, N and Moustafa, A. (2020). Industrial solid waste for heavy metals adsorption features and challenges; a review. *Journal of Materials Research and Technology*,*9*(5), 10235–10253. https://doi.org/10.1016/j.jmrt.2020.07.045

Somayeh, R., Albas, R., Muhammed, N.Z., Syed, S.S and Shahin, A. (2019). Synthesis and characterization of MgO supported Fe-Co-Mn nanoparticles with exceptionally high adsorption capacity for Rhodamine B dye.*Journal of Materials Research and Technology,* 41:2238 – 2249.

Sonal, S and Mishra, B. (2021). A comprehensive review on the synthesis and performance of different zirconium-based adsorbents for the removal of various water contaminants. *Chemical Engineering Journal*, 424, 130509. DOI:https://doi.org/10.1016/J.CEJ.2021.130509.

Sud, D., Mahajan, G. and Kaur, M.P. (2008) Agricultural Waste Material as Potential Adsorbent for Sequestering Heavy Metal Ions from Aqueous Solutions—A Review. *Bioresource Technology*, 99, 6017-6027. DOI:https://doi.org/10.1016/j.biortech.2007.11.064

World Health Organization (WHO) (2022). Almost 1 million people die every year due to lead poisoning, with more children suffering long-term health effects. Culled from https://www.who.int/news/item/23-10-2022-almost-1-million-people-die-every-year-due-to-lead-poisoning--with-more-children-suffering-long-term-health-effects.html. Posted on the 23 October 2022

Xu, X., Lin, L and Yang, H. (2022). Effects of Water Pollution on Human Health and Disease Heterogeneity: A Review. *Front. Environ. Sci*., 10. DOI:https://doi.org/10.3389/fenvs.2022.880246

Yadav, S., Yadav, A., Bagotia, N., Sharma, A. K., and Kumar, S. (2021). Adsorptive potential of modified plant-based adsorbents for sequestration of dyes and heavy metals from wastewater - A review. *Journal of Water Process Engineering*, 42, 102148. DOI: https://doi.org/10.1016/j.jwpe.2021.102148

Zaimee, M.Z.A.; Sarjadi, M.S and Rahman, M.L. (2021). Heavy Metals Removal from Water by Efficient Adsorbents. *Water*, 13:2659. DOI: https://doi.org/10.3390/w13192659

Zhao, X., Jiang, M and Zhang, W. (2022). The Impact of Environmental Pollution and Economic Growth on Public Health: Evidence From China. *Frontiers in Public Health*, 10. DOI:https://doi.org/10.3389/fpubh.2022.861157.

Zuorro, A.; Iannone, A.; Natali, S and Lavecchia, R. (2019). Green Synthesis of Silver Nanoparticles Using Bilberry and Red Currant Waste Extracts. *Processes*, 7, 193.